

Probabilistic Approach for Detection of High-Frequency Periodic Signals using an Event Camera

David El-Chai Ben-Ezra, Ron Arad, Ayelet Padowicz,
Israel Tugendhaft

June 26, 2024

Abstract

Being inspired by the biological eye, event camera is a novel asynchronous technology that pose a paradigm shift in acquisition of visual information. This paradigm enables event cameras to capture pixel-size fast motions much more naturally compared to classical cameras.

In this paper we present a new asynchronous event-driven algorithm for detection of high-frequency pixel-size periodic signals using an event camera. Development of such new algorithms, to efficiently process the asynchronous information of event cameras, is essential and being a main challenge in the research community, in order to utilize its special properties and potential.

It turns out that this algorithm, that was developed in order to satisfy the new paradigm, is related to an untreated theoretical problem in probability: let $0 \leq \tau_1 \leq \tau_2 \leq \dots \leq \tau_m \leq 1$, originated from an unknown distribution. Let also $\epsilon, \delta \in \mathbb{R}$, and $d \in \mathbb{N}$. What can be said about the probability $\Phi(m, d)$ of having more than d adjacent τ_i -s pairs that the distance between them is δ , up to an error ϵ ? This problem, that reminds the area of order statistic, shows how the new visualization paradigm is also an opportunity to develop new areas and problems in mathematics.

Keywords: Algorithm analysis, event camera, order statistics, pattern recognition.

AMS Subject Classification: 68W40, 68Q25, 68Q87, 60C05.

1 Introduction

Event camera is a bio-inspired sensor that does not give information about its whole field of view, but only about changes in it. Each pixel of an event camera is asynchronously independent and responds only when it feels a brightness change that reaches a predefined threshold. Hence, in contrast to standard cameras that sample the whole field of view in a certain sampling-rate and output a sequence of synchronous frames, event cameras provide data only when a certain pixel feels

a predefined change in the illumination, and the output is a list of asynchronous polarized "events" sorted by their timestamp. Just to make it clear: ideally, if nothing changes in the field of view, the output of an event camera will be empty, while the amount of data of a frame-based camera is independent with changes in the field of view. Event cameras come with some special properties: timestamp in resolution of microseconds, low latency, high dynamic range (over 120 dB), and low power consumption (see [1, 2] for review).

Regarding missions that require detection of pixel-size fast motions, event cameras enjoy a system engineering built-in advantage compared to frame-based camera: while classical cameras need to sample the whole field of view with high frame-rate and process a lot of redundant data in order to find the signal, event cameras just "wait" for it, and keep only the relevant information from the signal. For event camera, it does not matter if the motion is fast or slow, when it comes, the camera will respond to it. Hence, in such missions, the new paradigm can naturally be used to surpass the performance of frame-based cameras.

A classical mission of that type is the detection of high-frequency periodic signals. Going back to frame-based cameras, the common approach to distinguish between signals of a given frequency and random flickering is based on the use of Fourier transform. Using frame cameras, one needs to sample the signal at a rate higher than double the desired frequency (due to the Nyquist criterion). This approach works nicely when the desired signal is not too fast, and not too short. However, if the frequency of the signal is higher than ~ 1 kHz, then sampling it with a frame-based camera and analyzing it with this approach can become quite cumbersome, and if the signal is too short, say $1 \mu s$ long, one might miss it altogether, or at least a large portion of it, due to the inherent camera dead time. We got so used to this approach that it takes a bit of thinking in order to realize that using the deep theory of Fourier transform for this mission sounds like using a 5-kilo hammer in order to knock a nail.

The asynchronous bio-inspired paradigm of event cameras offers an approach that sounds much more natural and intuitive: to check whether the time difference between adjacent events in a certain pixel corresponds to the temporal-period of the desired frequency. This approach is inherently more intuitive as it is the way human vision works to detect repetitive signals. Adapting this approach to an event camera, one can easily surpass the 1 kHz limit, without missing short signals, as event-cameras do not have a dead time. This approach was implemented in [3] to show the potential of event cameras to track led markers blinking at high frequency (> 1 kHz) carried by a drone. For more applications of this approach see [4, 5]. For event driven Fourier transform approach see [6].

As event cameras work differently from frame-based cameras, a main challenge in unlocking their potential is to develop novel asynchronous event driven methods and algorithms to process their output (see [7, 8, 9, 10, 11, 12, 13, 14] for some examples). In this paper, we use the notion "time-surface" and present a new asynchronous event-based algorithm to distinguish between signals of a given frequency and random flickering, based on the aforementioned intuitive approach (see [15, 16, 17, 18, 19, 20] and [1] for more applications of the notion "time surface").

Regarding the work in [3], the algorithm and analysis presented in this paper

have a few advantages. The first is that using the method in this paper, one can approximate the probability for false alarm, something that was not dealt in [3], but is important for real world applications. This emphasises the importance of the presented probabilistic approach. The second is the simplicity of the method. With the method presented here, one can consider events of a single polarity. Specifically, we consider here only positive events. This is an advantage as in certain situations and for some types of event cameras, it is not always easy in practice to tune the thresholds of the camera to achieve good accuracy for both polarities. Regarding its decision making, another advantage is that the algorithm does not go over each pixel and check the signal. The detections list is generated incidentally through looping over the events. In other words, only the temporal dimension plays role in running the algorithm and locating the signal.

As mentioned in the abstract, the analysis of the algorithm boils down naturally to the theoretical interesting probabilistic problem of estimating the probability

$$\Phi(m, d) = P(\#\{j \mid |\tau_{j+1} - \tau_j - \delta| < \epsilon\} \geq d)$$

where $0 \leq \tau_1 \leq \tau_2 \leq \dots \leq \tau_m \leq 1$ are originated by an unknown distribution, $\epsilon, \delta \in \mathbb{R}$, and $d \in \mathbb{N}$. Quite surprisingly, as far as we know, this problem was not studied in the literature. We say that it is surprising, as the problem seems to be natural to be asked under the area of order statistic. This shows the potential of the new paradigm to develop new areas in pure mathematics.

In the paper, we present an analysis of the problem that can be practical in certain cases. However, an accurate treatment of the problem stays open, even in the simple case where the distribution is uniform. Our analysis uses basic tools in probability theory to approximate the function $\Phi(m, d)$ by the explicit expression

$$Q(m, d) = \sum_{l=d}^{m-1} \binom{m-1}{l} P(m)^l (1 - P(m))^{m-1-l}$$

where $P(m) = T^{m+1} \left(\frac{1}{(T + \delta - \epsilon)^{m+1}} - \frac{1}{(T + \delta + \epsilon)^{m+1}} \right)$.

Problem 1. Is there any explicit formula for $\Phi(m, d)$ when the distribution is uniform, or under any other assumptions on the distribution?

Problem 2. Estimate the difference between $\Phi(m, d)$ under certain assumptions on the distribution, and $Q(m, d)$, or any other explicit approximation of $\Phi(m, d)$.

At the end of the paper, we demonstrate the algorithm performance, using the presented analysis, and show how its decision making distinguishes between the periodic signals of streetlights flickering at 100 Hz, and other random signals during twilight, when many objects in the field of view are flickering as a result of sun glittering. This example inspires to use the idea behind the presented algorithm, not only for detection, but also for flicker removal (see [21] for a different method).

2 The Output of an Event Camera

Contrary to a frame-based camera, the output of an event camera does not consist of a synchronous series of matrices that describe the gray level of the pixels. Instead, it consists of an asynchronous list of “events” that are generated in the following way.

Any pixel of the camera “remembers” a certain reference value for the intensity of the light in the pixel. Then, the pixel measures continuously the change of the intensity of the light with relation to the reference value. When the intensity of the light changes enough, and the change reaches a predefined value, the pixel takes two actions:

1. It updates the reference value to the current intensity value.
2. Reports an “event” that contains the following information:
 - (a) The timestamp of the change, in resolution of microseconds.
 - (b) The coordinates of the pixel.
 - (c) The polarity of the event, namely, if the event was triggered by a positive change of the light or a negative one.

The list of the events, which is the output of the camera, is given to the user, sorted by the timestamps of the events.

As the output of an event camera is sparse and very different from the one of a frame-based camera, it requires development of novel approaches in order to exploit its properties and potential.

One common approach that can be found in the literature, is to take the special output of the camera, make artificial frames out of it, and apply classical algorithms based on the frame-based paradigm. However, this approach, conceptually, will lead to bad results in a few aspects, as delicate temporal information gets lost when the frames are made out of the events list, and artificial unnecessary information of zero values is added to the frames.

Instead, as mentioned in the introduction, one needs to develop event-based asynchronous algorithms to process the output. In the following chapter we are going to present such an algorithm, with the goal of periodic signals detection.

3 Description of the algorithm

As was stated in the introduction, we consider only the positive events of the output. However, depending on the application and context, one can take the negative events instead, or consider both polarities. Therefore, the input of the algorithm is the list of positive events generated by the event camera

$$L = \{(t_i, x_i, y_i) \mid i = 1, \dots, k\}$$

where t_i is the i -th event timestamp, (x_i, y_i) is its pixel coordinates, and k is the number of events. We define the two following variables, which we keep constant along the algorithm:

1. $\delta :=$ the period of the signal we are looking for.
2. $\epsilon :=$ the error we consider in the period of the signal. Typical value for this variable should be the expected rise time of the signal.

let u, v be the dimensions of the event camera pixel array. As mentioned in the introduction, we use the notion of "time surface". Namely, in the initialization of the algorithm, we define a $2D$ array of dimensions $u \times v$ which we initialize its entries arbitrarily to be some negative number, smaller than $-\delta - \epsilon$. We denote it by TS , and we update it along the algorithm to store the last timestamp of a positive event reported by each of the pixels. In addition, we define two $2D$ arrays of dimensions $u \times v$, initialized to zero, which we denote by $Total$ and $Periodic$. Now, using a for-loop going along $i = 1, \dots, k$, the algorithm implements 4 steps. Here are the first 3 of them:

1. $Total_{x_i, y_i} := Total_{x_i, y_i} + 1$.
2. If $|t_i - TS_{x_i, y_i} - \delta| < \epsilon$, then $Periodic_{x_i, y_i} := Periodic_{x_i, y_i} + 1$.
3. $TS_{x_i, y_i} := t_i$.

In order to present the final step, consider a certain pixel (x, y) and denote

$$m = Total_{x, y}, \quad n = Periodic_{x, y}$$

Now, if our recording is T seconds long, and the events reported by the pixel are due to the desired periodic signal, we expect n to get close to $\frac{T}{\delta}$ during the for-loop, or at least to be big enough so it will be unlikely to relate it to a random flickering signal. How big should it be? This is exactly what we are analyzing below. To formulate the problem, let $0 \leq \tau_1 \leq \tau_2 \leq \dots \leq \tau_m \leq T$ originated from an unknown distribution. For $d \in \mathbb{N}$, denote the probability

$$\Phi(m, d) = P(\#\{j \mid |\tau_{j+1} - \tau_j - \delta| < \epsilon\} \geq d) \quad (3.1)$$

Then, in general, Φ is monotonically decreasing as a function of d , $\Phi(m, 0) = 1$, and $\Phi(m, m) = 0$. Now, let q be the allowed probability for false alarm in one pixel. We note that in general, q should be much smaller than the allowed probability for false alarm in the whole field of view. Then, there exists a minimal D such that $\Phi(m, D) \leq q$. Now, let $0 \leq s_1 \leq s_2 \leq \dots \leq s_m \leq T$ be the timestamps of the events reported by the pixel (x, y) . Then

$$n = Periodic_{x, y} = \#\{j \mid |s_{j+1} - s_j - \delta| < \epsilon\}.$$

We would like to say that the signal reported by the pixel (x, y) is unlikely to relate to a random flickering if $n \geq D$, which is equivalent to the condition

$$\Phi(m, n) \leq q.$$

Denote another $2D$ array of dimensions $u \times v$, initialized to zero, by $Detected$, to indicate, for each pixel, whether, considering the information processed by the for-loop so far, the pixel detected the signal. Now, we can present the final step of the for-loop:

- If $\Phi(Total_{x,y}, Periodic_{x,y}) \leq q$ and $Detected_{x,y} = 0$, then add the pixel (x, y) to the list of detections and update the value of $Detected_{x,y}$ to 1.
- If $\Phi(Total_{x,y}, Periodic_{x,y}) > q$ and $Detected_{x,y} = 1$, then remove the pixel (x, y) from the list of detections and update the value of $Detected_{x,y}$ to 0.

We emphasize that this final step can be written as a fourth step in the for-loop itself and does not need to come afterwards. This way, the algorithm does not need to look for the signal in each pixel after the for-loop is done: the detections are found incidentally through the temporal event loop. The output of the algorithm is then a list of pixels in which a periodic signal of the desired frequency has been detected, considering all the events in the pixels during the T -seconds recording.

We do not know about accurate estimations of $\Phi(m, d)$ in the literature, even in simple cases, e.g. when the events are uniformly distribution originated. However, in the following we suggest a practical way to approximate its values in order to complete the decision making of the algorithm.

4 Suggested analysis

Assume that $0 \leq \tau_1 \leq \tau_2 \leq \dots \leq \tau_m \leq T$ are unknown distribution originated. We start with estimating the probability for the distance between two arbitrary subsequent τ_i -s to be close to δ up to an error ϵ . For this estimation, we assume that the appearance of the τ_i -s is exponentially distributed with a parameter λ . Under this assumption, and the assumption $\epsilon \leq \delta$, the probability we are looking for is given by the formula

$$\tilde{P}(\lambda) = \int_{\delta-\epsilon}^{\delta+\epsilon} \lambda e^{-\lambda s} \cdot ds = (e^{\lambda\epsilon} - e^{-\lambda\epsilon})e^{-\lambda\delta}.$$

However, as we do not know the value of λ , but we do know that between 0 and T we have m τ_i -s, we are weighting this probability by the probability of having m events given a Poisson distribution with parameter $\rho = \lambda T$. Hence, we estimate the desired probability by the formula

$$\begin{aligned} P &= \int_0^\infty \tilde{P}(\lambda) \cdot \frac{\rho^m e^{-\rho}}{m!} \cdot d\rho \\ &= T \int_0^\infty \frac{(\lambda T)^m (e^{-\lambda(T+\delta-\epsilon)} - e^{-\lambda(T+\delta+\epsilon)})}{m!} \cdot d\lambda \\ &= T^{m+1} \left(\frac{1}{(T+\delta-\epsilon)^{m+1}} - \frac{1}{(T+\delta+\epsilon)^{m+1}} \right). \end{aligned}$$

where the latter equality is yielded by using repeatedly the method of integration by parts.

Remark 3. Expanding P and \tilde{P} , one can see that if $\delta \ll T$, then $\tilde{P}(\frac{m+1}{T})$ gives a good approximation for P . This is not far from the intuitive sense that in high probability, the parameter λ is close to the value $\lambda = \frac{m}{T}$. Indeed, under the aforementioned assumptions we have

$$\begin{aligned}
P &= \frac{1}{\left(1 + \frac{\delta - \epsilon}{T}\right)^{m+1}} - \frac{1}{\left(1 + \frac{\delta + \epsilon}{T}\right)^{m+1}} \\
&= \sum_{k=0}^{\infty} \frac{(m+k)!}{(k! \cdot m!)} \left(\left(\frac{-\delta + \epsilon}{T}\right)^k - \left(\frac{-\delta - \epsilon}{T}\right)^k \right) \\
&\approx (m+1) \cdot \frac{2\epsilon}{T} + (m+2)(m+1) \cdot \frac{2\epsilon\delta}{T^2}
\end{aligned}$$

$$\begin{aligned}
\tilde{P} \left(\frac{m+1}{T} \right) &= e^{\frac{m+1}{T}(\epsilon - \delta)} - e^{\frac{m+1}{T}(-\epsilon - \delta)} \\
&= \sum_{k=0}^{\infty} \frac{(m+1)^k}{k!} \left(\left(\frac{-\delta + \epsilon}{T}\right)^k - \left(\frac{-\delta - \epsilon}{T}\right)^k \right) \\
&\approx (m+1) \cdot \frac{2\epsilon}{T} + (m+1)^2 \cdot \frac{2\epsilon\delta}{T^2}.
\end{aligned}$$

Notice now that given the information of having m events reported by the pixel, the probability for two adjacent events of the pixel to be close to each other in the appropriate distance is not independent. However, for the sake of simplicity we do not take into account this fact. Hence, the probability of at least d adjacent events out of $M = m - 1$ to be close to each other in the appropriate distance can be approximated by

$$Q(m, d) = \sum_{l=d}^{m-1} \binom{m-1}{l} P(m)^l (1 - P(m))^{m-1-l}.$$

In the sequent, we use $Q(m, d)$ as an approximation for the desired $\Phi(m, d)$ presented in Equation 3.1.

It is obvious that just like $\Phi(m, d)$, for any m , $Q(m, d)$ is monotonically decreasing as function of d . However, the dependence of $Q(m, d)$ on m is more tricky as the parameter m influences Q in two opposite directions. From one hand, when m grows it means that there are more events, and hence it should be easier to reach the threshold d , so Q should grow. On the other hand, when m grows, the event rate grows as well, and hence the chance for a specific random event to be far from the previous one in the right interval gets smaller, so P decreases, and hence Q should decrease also. This observation is summarized in the following proposition, showing that the function Q does encode these two opposite effects.

Proposition 4. *Given a specific value for the variables δ , ϵ , T , d , with $\epsilon \leq \frac{\delta}{2}$ and $d > 0$, one has:*

$$\lim_{m \rightarrow 0} Q(m, d) = \lim_{m \rightarrow \infty} Q(m, d) = 0.$$

In particular, Q reaches a maximum value as a function of m .

Proof. Writing $P = P(m)$ and using the assumption $d > 0$, one has

$$\begin{aligned}
Q(m, d) &= \sum_{l=d}^{m-1} \binom{m-1}{l} P^l (1-P)^{m-1-l} \\
&= P \cdot \sum_{l=d}^{m-1} \binom{m-1}{l} P^{l-1} (1-P)^{m-1-l} \\
&= P \cdot \sum_{l=d-1}^{m-2} \frac{m-1}{l+1} \binom{m-2}{l} P^l (1-P)^{m-2-l} \\
&\leq P \cdot m \cdot \sum_{l=d-1}^{m-2} \binom{m-2}{l} P^l (1-P)^{m-2-l} \\
&= P \cdot m \cdot Q(m-1, d-1) \leq P \cdot m \\
&= m \cdot T^{m+1} \left(\frac{1}{(T+\delta-\epsilon)^{m+1}} - \frac{1}{(T+\delta+\epsilon)^{m+1}} \right) \xrightarrow{m \rightarrow 0} 0.
\end{aligned}$$

As we assume that $\epsilon \leq \frac{\delta}{2}$, we have $\delta - \epsilon > 0$, and hence we also have

$$\begin{aligned}
Q(m, d) &\leq \frac{m \cdot T^{m+1}}{(T+\delta-\epsilon)^{m+1}} \\
&= \frac{m}{\left(1 + \frac{\delta-\epsilon}{T}\right)^{m+1}} \xrightarrow{m \rightarrow \infty} 0.
\end{aligned}$$

□

5 Demonstration

In general, the algorithm has better performance with detecting fast rising periodic signals, as in these cases one can choose the error parameter ϵ of the algorithm to be relatively small. However, in order to feel its effectiveness lower bound, we demonstrate it here on the periodic signal of a streetlight powered by sinusoidal current of the electrical grid. In this case, the rising time of the signal is basically half of the period. Hence, if we do not want to miss any of the events related to the periodic signal, we need to choose ϵ to its highest reasonable value, namely $\epsilon = \frac{\delta}{2}$. In this case, as the frequency of the signal is 100 Hz, we have $\delta = 10$ ms, and hence $\epsilon = 5$ ms.

Our experimental setup is built up of two cameras staring on approximately the same urban view: Prophesee Gen4 event-camera with resolution of 1M pixel, and a CMOS frame camera for guidance. Figure 5.1 shows the intersection of the two cameras field of view, seen by the frame camera. This intersection covers the field of view of approximately 1000×600 pixels of the event camera.

In Figure 5.1 we point out some well seen sun glittering coming from the buildings on the mountains, but there are also some intensive pixel size challenging sun glittering signals from the closer urban view that cannot be easily seen in the picture. We also point out the location of a streetlight.

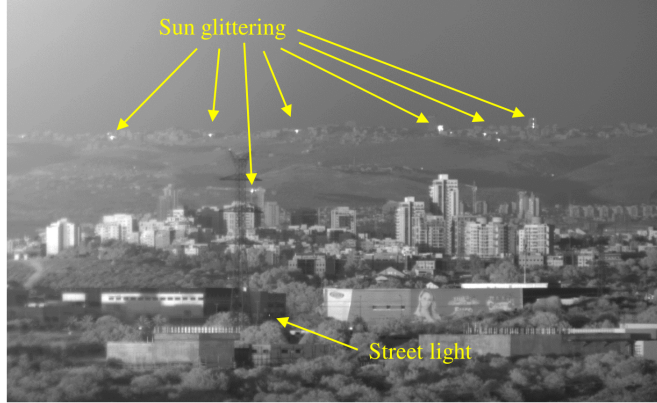


Figure 5.1: The intersection of the frame camera and event camera field of view.

Now, in order to demonstrate how the algorithm distinguishes between the periodic signal of the streetlight, and all the other events, we recorded one second of the scene, i.e. $T = 1 s$. Then, we applied the algorithm on the recording, and evaluated the function $Q(m, n)$ for each pixel.

The logarithmic graph in Figure 5.2 shows the number of pixels in the intersection field of view that reported more than 5 events during the recording, for which the probability function $Q(m, n)$ is smaller than the value of the allowed probability for false alarm given in the horizontal axis. In addition, it shows how many pixels out of them, are related to the periodic signal of the streetlight.

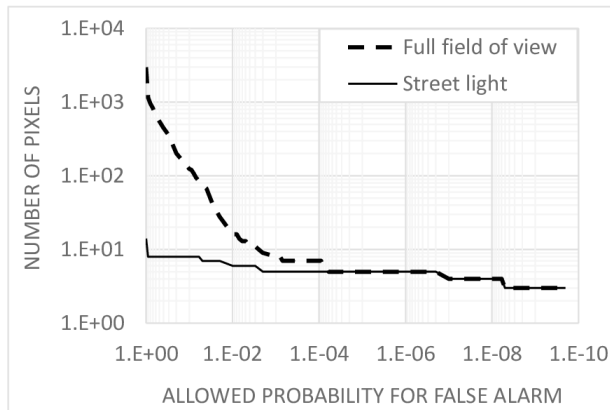


Figure 5.2: Number of pixels with probability function value smaller than the allowed probability for false alarm.

The graph shows that when the probability for false alarm is smaller than 10^{-5} , we remain with only 5 pixels that have enough events in the output of the algorithm, and all of them are related to the streetlight. Moreover, the value of the probability function of these 5 pixels is at least 2 orders of magnitude

less than 10^{-5} . In other words, there is a very clear dichotomy between the probability function of these 5 pixels and the one of the other pixels. Hence, these 5 pixels are very well distinguished by the algorithm and the analysis presented here.

One can also see in Figure 5.2 that there were additional 9 pixels that have reported more than 5 events during the recording, and their events are related to the streetlight, but were flickering more weakly, and hence the algorithm could not distinguish them effectively from other random signals. In Table 1 we give the values of the variables that were involved in evaluating the probability function of all the pixels that responded to the flickering street light: the 5 distinguished pixels and the other 9 with weak signal, sorted according to the value of the probability function.

Pixel	m	n	Q
1	554	99	$\sim 10^{-16}$
2	506	98	$\sim 2 \cdot 10^{-16}$
3	160	98	$\sim 3 \cdot 10^{-11}$
4	376	99	$\sim 6 \cdot 10^{-9}$
5	342	99	$\sim 10^{-7}$
6	132	66	$\sim 2 \cdot 10^{-3}$
7	188	76	$\sim 2 \cdot 10^{-2}$
8	89	41	$\sim 5 \cdot 10^{-2}$
9	26	2	~ 1
10	80	20	~ 1
11	96	24	~ 1
12	22	0	~ 1
13	10	0	~ 1
14	9	0	~ 1

Table 1: Variables of the pixels reacting to the signal of the streetlight.

Remark 5. By analyzing the periodic signals more carefully, one can find a better value for the error parameter ϵ , say $\epsilon = 3$ ms, and be able to add pixels 6-8 in Table 1 to the list of the distinguished pixels. We also remark that obviously, analyzing a longer recording can help to detect these pixels as well.

Remark 6. Concentrating on the 5 distinguished pixels, one can see that for all of them we have $98 \leq n \leq 99$ which is very close to the expected number $\frac{T}{\delta} = 100$, but m varies between $160 \leq m \leq 554$. The reason m is much higher than the expected number of events in the pixel, is that in each of the periods, the rise of the signal triggered more than one event: as powerful as the signal was, more events were triggered in each of the periods. Now, focusing on the relation between m and Q , one can see that Q reached a higher value when $m = 342$ (Pixel 5) than in the case $m = 160$ (Pixel 3). But after that, when we move from Pixel 5 to Pixel 4 and so on, when m grows, Q becomes smaller. This phenomenon demonstrates the validation of Proposition 4.

Ben-Ezra, David El-Chai, Remote Sensing Department, Soreq NRC, Yavne, Israel, 81800 (dbenezra@mail.huji.ac.il)

Arad, Ron, Remote Sensing Department, Soreq NRC, Yavne, Israel, 81800 (fnarad@yahoo.com)

Padowicz, Ayelet, Remote Sensing Department, Soreq NRC, Yavne, Israel, 81800 (ayeletp@soreq.gov.il)

Tugendhaft, Israel, Remote Sensing Department, Soreq NRC, Yavne, Israel, 81800 (tugen@soreq.gov.il)

References

- [1] G. Gallego, T. Delbruck, G. Orchard, C. Bartolozzi, B. Taba, A. Censi, S. Leutenegger, A. J. Davison, J. Conradt, K. Daniilidis and D. Scaramuzza, "Event-based Vision: A Survey," *IEEE transactions on pattern analysis and machine intelligence*, 44(1), 154-180, 2020.
- [2] M. H. Tayarani-Najaran and M. Schmuker, "Event-Based Sensing and Signal Processing in the Visual, Auditory, and Olfactory Domain: A Review," *Frontiers in Neural Circuits*, 15, 2021.
- [3] A. Censi, J. Strubel, C. Brandli, T. Delbruck and D. Scaramuzza, "Low-latency localization by Active LED Markers tracking using a Dynamic Vision Sensor," *2013 IEEE/RSJ International Conference on Intelligent Robots and Systems*, 891-898, 2013.
- [4] A. Mitrokhin, C. Fermüller, C. Paramehwara, and Y. Aloimonos, "Event-based moving object detection and tracking," *IEEE 2018 IEEE/RSJ International Conference on Intelligent Robots and Systems (IROS)*, 1-9, 2018.
- [5] D. Falanga, K. Kleber, and D. Scaramuzza. "Dynamic obstacle avoidance for quadrotors with event cameras," *Science Robotics* 5(40), eaaz9712, 2020.
- [6] Q. Sabatier, S.-H. Ieng and R. Benosman, "Asynchronous Event-Based Fourier Analysis," *IEEE Transactions on Image Processing*, 26(5), 2192-2202, 2017.
- [7] Z. Ni, C. Pacoret, R. Benosman, S. Ieng, S. RÉGNIER, "Asynchronous event-based high speed vision for microparticle tracking," *Journal of microscopy*, 245(3), 236-244, 2012.
- [8] X. Lagorce, C. Meyer, S. H. Ieng, D. Filliat, R. Benosman, "Asynchronous event-based multikernel algorithm for high-speed visual features tracking" *IEEE transactions on neural networks and learning systems*, 26(8), 1710-1720, 2014.

- [9] I. Alzugaray, M. Chli, ACE: An efficient asynchronous corner tracker for event cameras, *IEEE 2018 International Conference on 3D Vision (3DV)*, 653-661, 2018.
- [10] I. Alzugaray, M. Chli, “Asynchronous corner detection and tracking for event cameras in real time,” *IEEE Robotics and Automation Letters*, 3(4), 3177-3184, 2018.
- [11] R. Li, D. Shi, Y. Zhang, K. Li, R. Li, “Fa-harris: A fast and asynchronous corner detector for event cameras,” *2019 IEEE/RSJ International Conference on Intelligent Robots and Systems (IROS)*, 6223-6229, 2019.
- [12] H. Chen, Q. Wu, Y. Liang, X. Gao, H. Wang, “Asynchronous tracking-by-detection on adaptive time surfaces for event-based object tracking,” *Proceedings of the 27th ACM International Conference on Multimedia*, 473-481, 2019.
- [13] Z. Wang, T. Molloy, P. van Goor, R. Mahony, “Event Blob Tracking: An Asynchronous Real-Time Algorithm,” *arXiv:2307.10593*, 2023.
- [14] D. Gehrig, D. Scaramuzza, “Low-latency automotive vision with event cameras,” *Nature* 629(8014), 1034-1040, 2024.
- [15] R. Benosman, C. Clercq, X. Lagorce, S.-H. Ieng, and C. Bartolozzi, “Event-based visual flow,” *IEEE Trans. Neural Netw. Learn. Syst.*, 25(2), 407-417, 2014.
- [16] V. Vasco, A. Glover, and C. Bartolozzi, “Fast event-based Harris corner detection exploiting the advantages of event-driven cameras,” *IEEE Int. Conf. Intell. Robot. Syst. (IROS)*, 2016.
- [17] E. Mueggler, C. Bartolozzi, and D. Scaramuzza, “Fast event-based corner detection,” *British Mach. Vis. Conf. (BMVC)*, 2017.
- [18] A. Sironi, M. Brambilla, N. Bourdis, X. Lagorce, and R. Benosman, “HATS: Histograms of averaged time surfaces for robust eventbased object classification,” *IEEE Conf. Comput. Vis. Pattern Recog. (CVPR)*, 2018.
- [19] Y. Zhou, G. Gallego, H. Rebecq, L. Kneip, H. Li, and D. Scaramuzza, “Semi-dense 3D reconstruction with a stereo event camera,” *Eur. Conf. Comput. Vis. (ECCV)*, 2018.
- [20] J. Manderscheid, A. Sironi, N. Bourdis, D. Migliore, and V. Lepetit, “Speed invariant time surface for learning to detect corner points with event-based cameras,” *IEEE Conf. Comput. Vis. Pattern Recog. (CVPR)*, 2019.
- [21] Z. Wang, D. Yuan, Y. Ng, R. Mahony, “A linear comb filter for event flicker removal,” *2022 International Conference on Robotics and Automation (ICRA)*, 398-404, 2022.